Experimental moment resistance of rectangular hollow section T joints

Marsel Garifullin[1,*]

[1]Laboratory of Civil Engineering, Tampere University of Technology, FI-33720 Tampere, Finland

Abstract. Resistance is the main property of tubular joints. The determination of the joint resistance from the experimental load-deformation curve always represents a challenging task. Currently there are two main methods to find the experimental resistance, which are called plastic and ultimate resistance. However, there is no single opinion on which one should be commonly used. Based on the experimental results, this paper directly compares the two existed approaches. The study is restricted to welded square hollow section T joints under in-plane bending moment. The paper considers only the joints with $\beta < 0.85$, i.e. when the behaviour of the joint is governed by chord face failure. The results show that plastic resistance leads to more conservative results than ultimate resistance, providing thus safer results. However, attention should be also paid to the difference between the labour intensity of the presented methods.

1 Introduction

Welded tubular joints are met in a wide range of trusses and frames, leading to nice appearance and excellent structural behaviour. In such structures, rectangular hollow section (RHS) joints combine great structural properties and simple welding process [1]. A T joint represents the simplest joint configuration, when a brace is welded to a chord at an angle of 90°, as shown in Fig. 1a. The main properties of this joint are the dimensions of the chord (b_0, h_0, t_0) and the brace (b_1, h_1, t_1). Another important parameters of the joint are the brace-to-chord width ratio $\beta = b_1 / b_0$ and the throat thickness of the fillet weld a_w.

A comprehensive research on tubular joints was conducted by Wardenier [2]. Later, the behaviour of tubular joints under in-plane bending moment was considered in [3–5], under axial loading in [6–8]. An extensive research on RHS joints was carried out by Yu [9]. The influence of chord axial stresses on the behaviour of joints was investigated in [10]. The behaviour of RHS T joints with initial imperfections was investigated in [11, 12]. Currently, the equations of Wardenier are employed in many design standards, including EN 1993-1-8:2005 [13] and CIDECT Design Guide [14].

The behaviour of tubular joints can be described using a load-deformation curve, as depicted in Fig. 1b. The structural properties of RHS T joints, such as initial stiffness and resistance, are determined from this curve [15–17]. In the beginning of the loading, the joint

* Corresponding author: marsel.garifullin@tut.fi

demonstrates elastic behaviour and is characterized by initial stiffness $S_{j,ini}$ ($C_{j,ini}$). As the stresses in the joint reach the yield strength of steel, chord face bending starts to develop, followed by a noticeable decline in the slope [2]. However the joint continues resist the load, and the curve exhibits a clearly observed hardening phase, which is characterized by so-called hardening (membrane) stiffness $S_{j,h}$ ($C_{j,h}$). When the joint cannot resist any more load, it fails by the cracking in the weld, which corresponds to the maximum load M_{max} (N_{max}).

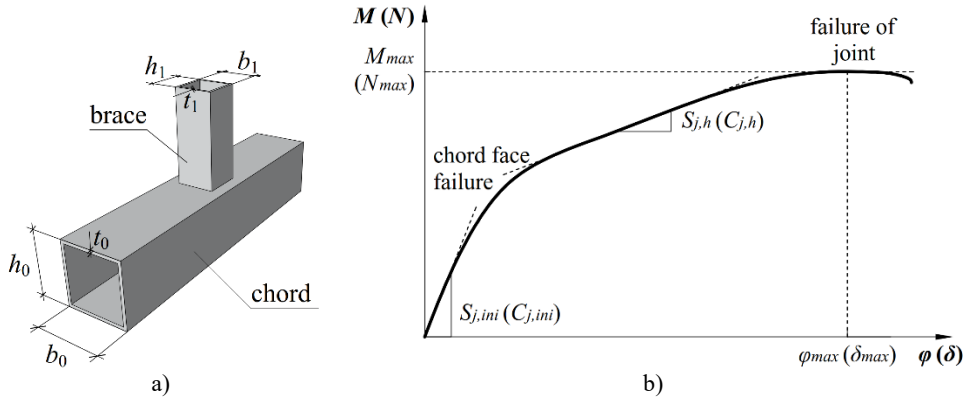

Fig. 1. RHS T joint: a) notations; b) load-deformation curve.

As can be seen, the determination of joint resistance from this curve is not evident and represents a challenging issue for scientists. Obviously, the maximum load corresponds to very large deformations φ_{max} (δ_{max}); therefore, it cannot be considered as the resistance of the joint, violating the serviceability limit state [18].

Generally, the scientific society presents two options to determine the resistance of tubular joints. The first one approximates the load-deformation curve by two straight lines adjusted to initial and hardening stiffnesses [19, 20, 7]. In this case, the plastic resistance M_{pl} (N_{pl}) is determined as the intersection of these two lines, as demonstrated in Fig. 2.

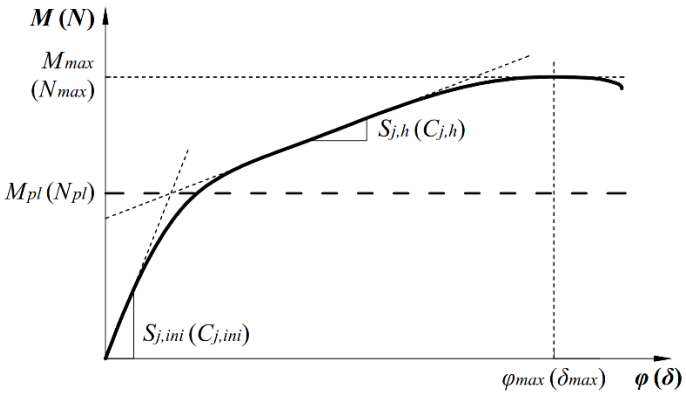

Fig. 2. Plastic resistance of T joint.

The second method was invented by Zhao [21], based on the 3%b_0 deformation limit, developed by Lu et al. [22]. This limit restricts the deformation of the tubular joint to 3% of its chord width b_0. The resistance of the joint is called ultimate resistance and it depends on the ratio of the ultimate load $N_{3\%b0}$ to the serviceability load $N_{1\%b0}$. If the ratio is less than 1.5, the ultimate resistance is determined as $N_{3\%b0}$, as demonstrated in Fig. 3a. If the ratio exceeds 1.5, the ultimate resistance is taken as $1.5N_{1\%b0}$, as illustrated in Fig. 3b. This procedure was

developed for axially loaded joints; however, it can be also extended to joints under in-plane bending due to the similarities between these loading cases.

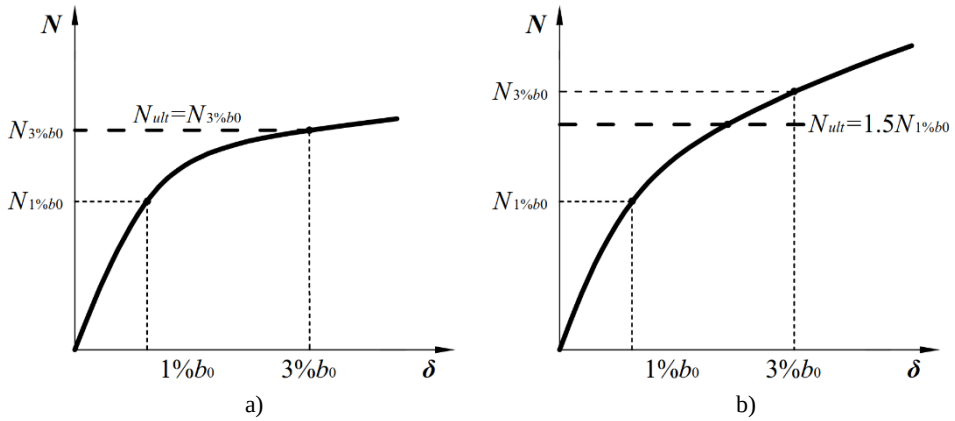

Fig. 3. Ultimate resistance of T joint: a) $N_{3\%b0}$ / $N_{1\%b0}$ <1.5; b) $N_{3\%b0}$ / $N_{1\%b0}$ >1.5.

Currently, there is no single opinion regarding the most suitable approach to determine the resistance of tubular joints. Based on the existing experimental results, this paper provides a short comparative analysis between the two presented methods. The aim of the paper is to determine which if the approached provides more conservative results and can be recommended for the theoretical design. The study is conducted only for RHS T joints under in-plane bending moment. Only the joints with $\beta \leq 0.85$ are considered, meaning that chord face bending governs the deformation of the whole joint [13].

2 Experimental investigation

The research considers the tests conducted in [23]. The specimens represent square hollow section T joints under in-plane bending moment, as shown in Fig. 4a. The brace was welded at the midpoint of the chord, as shown in Fig. 4b. The length of both the chord and the brace was equal to 700 mm. The brace-to-chord width ratio β varied from 0.67 to 0.80. Three steel grades were analysed: S420, S500 and S700. Three weld types were considered, a6 and a10 fillet welds and 1/2v butt welds. The details of the tested joints are collected in Table 1, where the specimens are named in the format [chord steel]_[brace steel]_[weld type]. Index *WiPF* denotes robot welding. All the tests were performed until the failure of the specimens. A moment-rotation curve was obtained for each joint.

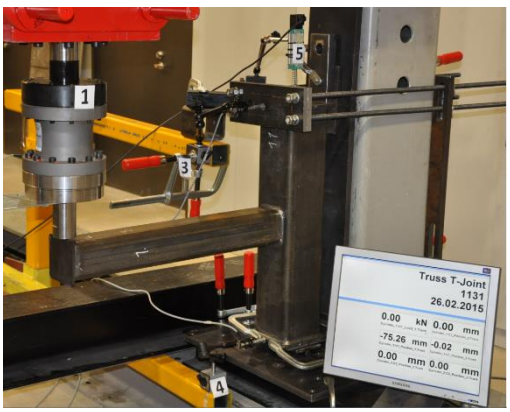

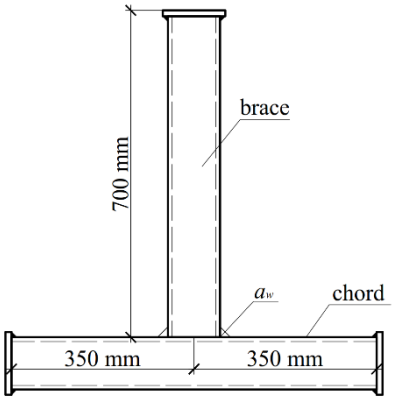

a) b)

Fig. 4. Experimental study: a) test setup; b) scheme of the specimen.

Table 1. Details of joints.

Joint	b_0 [mm]	h_0 [mm]	t_0 [mm]	Chord Steel	b_1 [mm]	h_1 [mm]	t_1 [mm]	β	Brace Steel	a_w [mm]
S420_S420_a6	150	150	8	S420	100	100	8	0.67	S420	6
S500_S420_a6				S500	100	100	8	0.67	S420	
S500_S500_a6				S500	100	100	8	0.67	S500	
S700_S420_a6				S700	100	100	8	0.67	S420	
S700_S500_a6				S700	100	100	8	0.67	S500	
S700_S500_a6_WiPF				S700	100	100	8	0.67	S500	
S700_S700_a6				S700	120	120	8	0.80	S700	
S420_S420_a10	150	150	8	S420	100	100	8	0.67	S420	10
S500_S420_a10				S500	100	100	8	0.67	S420	
S500_S500_a10				S500	100	100	8	0.67	S500	
S700_S420_a10				S700	100	100	8	0.67	S420	
S700_S500_a10				S700	100	100	8	0.67	S500	
S700_S500_a10_WiPF				S700	100	100	8	0.67	S500	
S700_S700_a10				S700	120	120	8	0.80	S700	
S420_S420_1/2v	150	150	8	S420	100	100	8	0.67	S420	1/2v
S500_S420_1/2v				S500	100	100	8	0.67	S420	
S500_S500_1/2v				S500	100	100	8	0.67	S500	
S700_S420_1/2v				S700	100	100	8	0.67	S420	
S700_S500_1/2v				S700	100	100	8	0.67	S500	
S700_S700_1/2v				S700	120	120	8	0.80	S700	

3 Results and Discussion

The plastic M_{pl} and ultimate M_{ult} resistance was determined for every joint from its moment-rotation curve and summarized in Table 2. As can be seen, ultimate resistance exceeds plastic resistance for all the joints. The ratio M_{ult} / M_{pl} remains in the range from 1.07 to 1.22 with the average value of 1.16. The smallest ratios M_{ult} / M_{pl} are observed for the cases S700_S700_a6, S700_S700_a10 and S700_S700_1/2v. These joints have nominal $\beta = 0.80$; however, fillet welds increase the ratio β, making it close to 0.85 and even greater [24], particularly in case S700_S700_a10. For these reason, these joints behave similar to those with $\beta > 0.85$ and demonstrate a very inconsiderable hardening phase. In general, these findings show that plastic resistance is 16% more conservative in comparison to ultimate resistance. An example is presented in Fig. 5a for joint S500_S420_a6.

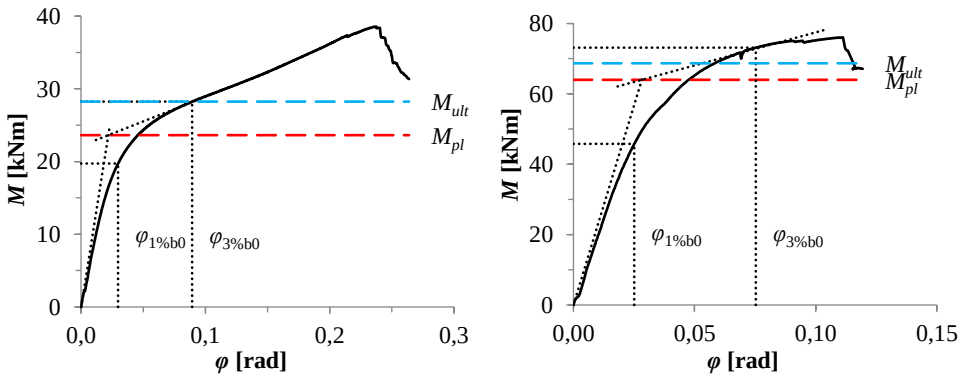

a) b)

Fig. 5. Moment-rotation curves: a) joint S500_S420_a6; b) joint S700_S700_a10.

Table 2. Comparison between plastic and ultimate resistance.

Joint	β	$M_{1\%b0}$ [kNm]	$M_{3\%b0}$ [kNm]	$M_{3\%b0}$ / $M_{1\%b0}$	M_{ult} [kNm]	M_{pl} [kNm]	M_{ult} / M_{pl}
S420_S420_a6	0.67	18.2	24.8	1.36	24.8	20.5	1.21
S500_S420_a6	0.67	19.7	28.2	1.43	28.2	23.6	1.20
S500_S500_a6	0.67	20.6	29.2	1.41	29.2	24.7	1.18
S700_S420_a6	0.67	21.8	32.7	1.50	32.7	27.1	1.21
S700_S500_a6	0.67	22.7	33.8	1.49	33.8	28.9	1.17
S700_S500_a6	0.67	23.6	35.5	1.50	35.5	30.4	1.17
S700_S700_a6	0.80	44.0	64.3	1.46	64.3	59.0	1.09
S420_S420_a10	0.67	27.5	36.4	1.32	36.4	31.8	1.14
S500_S420_a10	0.67	29.0	39.9	1.38	39.9	34.9	1.14
S500_S500_a10	0.67	29.6	41.2	1.39	41.2	37.3	1.10
S700_S420_a10	0.67	30.7	44.0	1.43	44.0	38.5	1.14
S700_S500_a10	0.67	36.2	51.0	1.41	51.0	45.7	1.11
S700_S500_a10	0.67	29.1	42.5	1.46	42.5	37.0	1.15
S700_S700_a10	0.80	45.8	73.1	1.60	68.7	64.0	1.07
S420_S420_1/2v	0.67	16.1	21.9	1.36	21.9	18.2	1.20
S500_S420_1/2v	0.67	17.7	24.8	1.40	24.8	20.9	1.19
S500_S500_1/2v	0.67	18.3	24.8	1.36	24.8	20.4	1.22
S700_S420_1/2v	0.67	18.9	28.6	1.51	28.4	23.4	1.21
S700_S500_1/2v	0.67	20.4	30.3	1.49	30.3	25.6	1.18
S700_S700_1/2v	0.80	35.3	50.0	1.42	50.0	44.7	1.12
Average							**1.16**

Attention should be also paid to the practical aspects. The determination of plastic resistance requires considerable efforts to numerically construct the tangent lines and find their intersection. Moreover, for some joints the construction of tangent lines is not evident and allows several solutions, reducing the accuracy of the procedure, as demonstrated in Fig. 5b for joint S700_S700_a10. In comparison to this, the determination of ultimate resistance is more exact and straightforward and requires considerably less computational efforts.

4 Conclusions

The paper compared the two approaches that currently exist for the determination of the resistance of tubular joints from load-deformation curves. The comparison was based on the experimental results on square hollow section T joints with $\beta < 0.85$ under in-plane bending. The results demonstrated that ultimate resistance exceeded plastic resistance for all the joints, by 16% in average. As expected, the difference was smaller for the joints with high β. From that point of view, it can be concluded that plastic resistance represents more conservative and thus safer results than ultimate resistance, requiring, however, considerably more computational efforts.

References

1. M.N. Kirsanov, Mag. Civ. Eng., **1** (2015)
2. J. Wardenier, *Hollow section joints* (Delft University of Technology, Delft, 1982)

3. A.D. Christitsas, D.T. Pachoumis, C.N. Kalfas, E.G. Galoussis, J. Constr. Steel Res., **63** (**10**) (2007)
4. J. Szlendak, Thin-Walled Struct., **12** (**1**) (1991)
5. J.A. Packer, J. Constr. Steel Res., **25** (**1**–**2**) (1993)
6. A. Nizer, L.R.O. de Lima, P.C.G.S. Vellasco, S.A.L. de Andrade, E. da S. Goulart, A.T. da Silva, L.F. Costa-Neves, Steel Constr., **9** (**4**) (2016)
7. X.L. Zhao, G.J. Hancock, J. Struct. Eng., **117** (**8**) (1991)
8. J. Becque, T. Wilkinson, J. Constr. Steel Res., **133** (2017)
9. Y. Yu, *The static strength of uniplanar and multiplanar connections in rectangular hollow sections* (Delft University of Technology, Delft, 1997)
10. A. Lipp, T. Ummenhofer, *Tubular Structures XV: Proceedings of the 15th International Symposium on Tubular Structures, Rio de Janeiro, Brazil, 27-29 May 2015* (Taylor & Francis Group, London, 2015)
11. M. Garifullin, M. Bronzova, M. Heinisuo, K. Mela, S. Pajunen, Mag. Civ. Eng., **4** (2018)
12. N.I. Vatin, T. Nazmeeva, R. Guslinscky, Adv. Mater. Res., **941**–**944** (2014)
13. CEN, *Eurocode 3: Design of steel structures – Part 1-8: Design of joints (EN 1993-1-8:2005)* (Brussels, 2005)
14. J.A. Packer, J. Wardenier, X.L. Zhao, G.J. van der Vegte, Y. Kurobane, *Design guide for rectangular hollow section (RHS) joints under predominantly static loading. CIDECT Design Guide No. 3* (LSS Verlag, 2009)
15. L.A.P. Silva, L.F.N. Neves, F.C.T. Gomes, J. Struct. Eng., **129** (**4**) (2003)
16. O.A. Tusnina, A.I. Danilov, Mag. Civ. Eng., **4** (2016)
17. A.R. Tusnin, M. Prokic, Mag. Civ. Eng., **1** (2015)
18. X.L. Zhao, J. Wardenier, J.A. Packer, G.J. van der Vegte, Proc. Inst. Civ. Eng. — Struct. Build., **163** (**6**) (2010)
19. M. Garifullin, N. Vatin, T. Jokinen, M. Heinisuo, *Advances and Trends in Engineering Sciences and Technologies II - Proceedings of the 2nd International Conference on Engineering Sciences and Technologies, ESaT 2016* (Taylor & Francis Group, London, 2017)
20. D. Grotmann, G. Sedlacek, *Rotational stiffness of welded RHS beam-to-column joints. Cidect 5BB-8/98* (RWTH-Aachen, Aachen, 1998)
21. X.L. Zhao, J. Constr. Steel Res., **53** (**2**) (2000)
22. L.H. Lu, G.D. de Winkel, Y. Yu, J. Wardenier, *Tubular Structures VI, 6th International Symposium on Tubular Structures, Melbourne, Australia* (Balkema, Rotterdam, 1994)
23. J. Havula, M. Garifullin, M. Heinisuo, K. Mela, S. Pajunen, Eng. Struct., **172** (2018)
24. M. Garifullin, M. Bronzova, T. Jokinen, M. Heinisuo, B. Kovačič, Procedia Eng., **165** (2016)